British Journal of Mathematics & Computer Science

22(6): 1-13, 2017; Article no.BJMCS.34222
ISSN: 2231-0851

Comparison of State-Estimation Algorithms for a Noise-Injected Lithium-ion Battery System

Hasan A. Bjaili[1*], Ali M. Rushdi[1] and Muhammad Moinuddin[1]

[1] *Department of Electrical and Computer Engineering, King Abdulaziz University, PO Box 80204, Jeddah 21589, Saudi Arabia.*

Authors' contributions

This work was carried out in collaboration between all authors. Author HAB designed the study, managed literature survey, performed the analysis, implemented the algorithm, drew the figures and wrote the first draft of the manuscript. Author AMR contributed to the literature review and contributed to the analysis. Author MM reviewed and proofed the study and algorithm. All authors read and approved the final manuscript.

Article Information

DOI: 10.9734/BJMCS/2017/34222
Editor(s):
(1) Mehmet Sirin Demir, Department of Mechanical Engineering, Faculty of Engineering, A/7, Istanbul University, Avcilar Campus 34320 Istanbul, Turkey.
Reviewers:
(1) Wen-Yeau Chang, St. Johns University, Taiwan.
(2) Ho Pham Huy Anh, University of Technology, Vietnam.
(3) Sofiya Ostrovska, Atilim University, Turkey.
Complete Peer review History: http://www.sciencedomain.org/review-history/19645

Received: 18th May 2017
Accepted: 13th June 2017
Published: 22nd June 2017

Original Research Article

Abstract

This paper deals with one of the most prominent problems in industrial prognostics, namely the estimation of the Remaining Useful Life (RUL) of the most popular industrial battery, *viz.*, the lithium-ion battery. The paper presents a state-space model of the battery, and then estimates the dynamic behavior of seven of its process variables and two of its sensor variables. The estimation is achieved *via* two well known estimators, the Unscented Kalman Filter (UKF) and the Particle Filter (PF) when noise of various levels and types is injected. Numerical and chart comparisons of these two computing estimators are reported and discussed.

Keywords: Prognostics; state-space modeling; Remaining Useful Life (RUL), lithium-ion battery; reliability.

**Corresponding author: E-mail: hasan@bjaili.com, halbjaili@stu.kau.edu.sa;*

1 Introduction

The lithium-ion battery is the most prominent kind of batteries in modern applications. Constant improvement to the battery efficiency, lower cost of production and increased power density led to spread and advancement of many systems such as electric cars, smart-phones, aircraft and satellites communications. The aforementioned systems are an essential part of our contemporary lives. Hence, it was necessary to develop means of predicting when the battery will cease operation and stop working. Therefore, predicting the Remaining Useful Life (RUL) (also known as the Mean Residual Life (MRL)) became a major concern to various industries that rely on batteries [1]. This has motivated many scientists to develop an accurate model of the battery and its capabilities [2]. For years, industry kept a good record of these batteries capabilities [3] to predict the End-of-Discharge (EOD) and End-of-Life (EOL) precisely [4, 5].

It is very crucial to accurately monitor the health of batteries, especially for battery-powered vehicles, as they could cause a lot of damages if they go bad during operation [6, 7]. For example, the Boeing Dreamliner (B787) aircraft Auxiliary Power Unit (APU) caught a fire causing the whole fleet to be grounded [8]. A thermal runaway condition was not detected by the battery monitoring system. In 2006, the National Aeronautics and Space Administration (NASA) has lost significant amount of its Mars Global Surveyor capacity due to battery overheating. Both the Mars Viking II Lander as well as the Air Force Research Laboratory (AFRL) Advanced Research and Global Observation Satellite (ARGOS) had their batteries failed, which led to the termination of the mission of each satellite.

The aforementioned anomalies could have been prevented should we have had a good and advanced health monitoring system [9]. In order to implement a good battery health monitoring system, an accurate understanding of its function should be captured in the form of a model which can be used by the monitoring and prognostics algorithms. Once an accurate model is developed, it will be fairly easy to predict and detect all pertinent battery events, including its State-of-Charge (SOC) [10, 11], State-of-Health (SOH), End-of-Discharge (EOD) and End-of-Life (EOL). The EOD event, in particular, is determined directly by the battery age. An old battery will discharge faster than a new one because its capacity is diminished over time [4, 9]. Few researchers have studied the battery underlying process and dynamics [12, 13]. However, only few attempts were made to perform battery estimation online and in real time [4]. In [9], the authors measured the capacity of the battery over a sequence of reference discharge cycles, and fitted some empirical formulas on them. Once fitting is achieved, capacity is measured by determining the time t the battery takes to reach a voltage threshold which defines the EOD. The battery capacity is calculated in Ampere hour (Ah) by multiplying the reference discharge current by the time t [14]. This whole method of measuring the battery capacity relies on the reference current. The battery Ah rating will be low when the reference current is increased and high when the reference current is decreased. This means that the relationship between the discharge current and discharge time is non-linear; in fact, as inverse one. The apparent capacity will increase if the battery is allowed enough time to rest between discharge cycles. Therefore, there are two fundamental issues with this approach.

1. The measurement of the capacity in such a way is not an accurate representation or indication of the battery age because the Ah rating depends on the current, temperature and other factors which can not be held constant in practical life.
2. In real life, the reference discharge is rather complex and is not readily available.

This paper presents a state-space model of the battery, and then estimates the dynamic behavior of seven of its process variables and two of its sensor variables. The estimation is achieved *via* two well known estimators, the Unscented Kalman Filter (UKF) and the Particle Filter (PF) when noise of various levels and types is injected. The Unscented Kalman Filter (UKF) is an improvement to the Extended Kalman Filter (UKF) which does not require using a differentiation as it is the

case with EKF. In addition to that, the UKF provides superior performance to the EKF in a similar computational environment. The UKF consists of *model forecast* and *data assimilation*. The idea behind the UKF is its ability to use probability distribution approximation rather than the approximation of an arbitrary nonlinear function or transformation [15, 16, 17].

The Particle Filter is a sequential Monte Carlo statistical simulation technique which can provide a very accurate approximation of the sequential Bayesian estimator [18]. The basic concept of particle filters as in [19] are described next. We use a set of weighted particles as follows:

$$\left\{w_{k-1}^{(i)}, \mathbf{x}_{k-1}^{(i)}\right\}_{i-1}^{N} \tag{1.1}$$

Where $\mathbf{x}_{k-1}^{(i)}$ is the state of the particle i and $w_{k-1}^{(i)}$ is its weight. These are used to approximate the posterior density at a time $k-1$. The weights are normalized, *i.e.*, $\sum_{i=1}^{N} w_{k-1}^{(i)} = 1$. The filter approximation, then, can be expressed as:

$$p\left(\mathbf{x}_{k-1}|\mathbf{z}_{1:k-1}\right) \approx \sum_{i=1}^{N} w_{k-1}^{(i)} \delta_{\mathbf{x}_{k-1}^{(i)}}\left(\mathbf{x}_{k-1}\right) \tag{1.2}$$

Where $\delta_{\mathbf{a}}(\mathbf{x})$ is the Dirac delta function or distribution that is concentrated at $\mathbf{a}$ and $\mathbf{z}_{1:k-1}$ is available measurements up to time $k-1$. Prognostics using Particle filtering and particle filters are described in detail in [20, 21, 9, 22, 23].

In passing, we stress that we deliberately limited the scope of our comparison by restricting it to just two types of model-based estimation algorithms. However, there are many other prominent such algorithms including Luenberger observers, sliding-mode observers, Extended Kalman Filters and Sigma-point Kalman Filters [24]. Other candidate algorithms include well-known heuristic algorithms, such as artificial neural-network (ANN) algorithms, genetic algorithm (GA), particle swarm optimization (PSO), tabu search (TS), and simulated annealing (SA), as well as meta-heuristic algorithms such as improved particle swarm optimization (IPSO), improved harmony search (IHS), improved harmony search-based simulated annealing (IHSBSA), and artificial bee swarm optimization (ABSO) [25]. There are many excellent expositions and reviews on the current topic of this paper and related issues [26, 27, 28, 29, 30].

The organization of the remainder of this paper is as follows. Section 2 reviews the concept and equations of the dynamical or state-space model with a stress on that of a Li-ion battery. Section 3 explains the setup of our simulations, and then reports and discusses their results. Section 4 concludes the paper.

2 State-Space Model

A state-space model, also known as a dynamical model, is a mathematical representation of a set of differential equations or difference equations. These equations represent a process x which is then expressed by a numerical vector. Two models represent the state-space model: the *process model* and the *measurement model*. The process model x characterizes the propagation in time based on external influences such as input and noise. The measurement model y simulates measurements which might be noisy and/or inaccurate. Although the battery model is non-linear, we begin our work by defining the general model of a linear time varying system:

$$\boldsymbol{x}[k+1] = \boldsymbol{A}[k]\boldsymbol{x}[k] + \boldsymbol{B}[k]\boldsymbol{u}[k] + \boldsymbol{w}[k], \tag{2.1a}$$

$$\boldsymbol{y}[k] = \boldsymbol{C}[k]\boldsymbol{x}[k] + \boldsymbol{D}[k]\boldsymbol{u}[k] + \boldsymbol{v}[k], \tag{2.1b}$$

where $\boldsymbol{x} \in \Re^n$ is the process state vector, $\boldsymbol{A}$ is the state transition matrix with dimensions of $n \times n$, $\boldsymbol{B}$ is the control matrix with dimensions of $n \times p$, $\boldsymbol{u} \in \Re^p$ is the input vector, $\boldsymbol{w} \in \Re^n$ is the process noise vector, $\boldsymbol{y} \in \Re^m$ is the measurement output vector such that $m \leq n$, $\boldsymbol{C}$ is the output matrix with dimensions of $m \times n$, $\boldsymbol{D}$ is the feed through matrix with dimensions of $m \times p$ and $\boldsymbol{v} \in \Re^m$ is the measurement noise vector.

Generally, the nonlinear continuous time system can be represented by Equations (2.2) and (2.3) where f and h are nonlinear functions:

$$\dot{\boldsymbol{x}} = f(\boldsymbol{x}, \boldsymbol{u}, \boldsymbol{w}), \tag{2.2}$$

$$\boldsymbol{y} = h(\boldsymbol{x}, \boldsymbol{u}, \boldsymbol{v}). \tag{2.3}$$

The Lithium-ion battery model can be represented as [4, 3, 14]:

$$\dot{E}_o = (V_o - E_o)/\tau_o, \tag{2.4}$$

$$\dot{E}_{\eta n} = (V_{\eta n} - E_{\eta n})/\tau_{\eta n}, \tag{2.5}$$

$$\dot{E}_{\eta p} = (V_{\eta p} - E_{\eta p})/\tau_{\eta p}, \tag{2.6}$$

$$\dot{q}_{bn} = -\dot{q}_{bsn}, \tag{2.7}$$

$$\dot{q}_{sn} = -i + \dot{q}_{bsn}, \tag{2.8}$$

$$\dot{q}_{bp} = -\dot{q}_{bsp}, \tag{2.9}$$

$$\dot{q}_{sp} = i + \dot{q}_{bsp}, \tag{2.10}$$

where $\dot{E}_{\eta p}$ and $\dot{E}_{\eta n}$ are the positive and negative voltage drops due to surface overpotential, $\dot{E}_o$ is the solid-phase ohmic-resistance voltage and the subscripted q symbols denote amounts of charge in the electrodes (positive p and negative n) where each is split into two volumes, surface layer s and bulk layer b. The overall voltage (output) of the system (battery) is characterized by Equation (2.11):

$$V(t) = V_{Up} - V_{Un} - E_o - E_{\eta p} - E_{\eta n} \tag{2.11}$$

In the state-space Equations (2.4) to (2.10) and the output Equation (2.11), i is the applied current and the following are the description and derivation of the related equations.

$$\dot{q}_{bsp} = \frac{1}{D}\left(\frac{q_{bp}}{v_{bp}} - \frac{q_{sp}}{v_{sp}}\right), \tag{2.12}$$

$$\dot{q}_{bsn} = \frac{1}{D}\left(\frac{q_{bn}}{v_{bn}} - \frac{q_{sn}}{v_{sn}}\right), \tag{2.13}$$

where $\dot{q}_{bsp}$ and $\dot{q}_{bsn}$ describe bulk to surface diffusion for the positive and negative electrodes and D is the diffusion constant.

The output Equation (2.11) is the sum of several electrochemical potentials and can be described as follows:

$$V_{Up} = U_0 + \frac{RT}{nF} ln\left(\frac{1 - x_{sp}}{x_{sp}}\right) + \frac{1}{nF}\left(\sum_{k=0}^{Np} A_{pk}\left((2x_p - 1)^{k+1} - \frac{2x_p k(1 - x_p)}{(2x_p - 1)^{1-k}}\right)\right), \tag{2.14}$$

$$V_{Un} = U_0 + \frac{RT}{nF} ln\left(\frac{1 - x_{sn}}{x_{sn}}\right) + \frac{1}{nF}\left(\sum_{k=0}^{Nn} A_{nk}\left((2x_n - 1)^{k+1} - \frac{2x_n k(1 - x_p)}{(2x_n - 1)^{1-k}}\right)\right), \tag{2.15}$$

where V_{Up} and V_{Up} are the equilibrium potential at the positive and negative current collectors.

$$V_o = iR_o, \tag{2.16}$$

$$V_{\eta p} = \frac{RT}{F\alpha} sinh^{-1}\left(\frac{i}{S_p k_p (1-x_{sp})^{\alpha}(x_{sp})^{1-\alpha}}\right), \tag{2.17}$$

$$V_{\eta n} = \frac{RT}{F\alpha} sinh^{-1}\left(\frac{i}{S_n k_n (1-x_{sn})^{\alpha}(x_{sn})^{1-\alpha}}\right), \tag{2.18}$$

3 Simulation and Results

In this section, we simulate and validate the performance of the Unscented Kalman Filter (UKF) [15, 31, 32, 33, 34] and Particle Filter (PF) [19, 20, 21, 22, 23] used to state estimate Lithium-ion Battery in [4] in the presence of noise in both the process (state) and the sensor (input) variables. The injected noise is listed in table 1.

Table 1. Four groups of noise injections

Process (State)	Group 1 (dB)	Group 2(dB)	Group 3 (dB)	Group 4 (dB)
$\dot{E}_o$	–60	–70	–80	–90
$\dot{E}_{\eta n}$	–60	–70	–80	–90
$\dot{E}_{\eta p}$	–60	–70	–80	–90
$\dot{q}_{bn}$	10	0	–10	–20
$\dot{q}_{sn}$	–10	–20	–30	–40
$\dot{q}_{bp}$	10	0	–10	–20
$\dot{q}_{sp}$	–10	–20	–30	–40
Sensor (Input)				
T_b	10	0	–10	–20
V	10	0	–10	–20

We inject three different types of process and sensor noise (*Gaussian*, *Uniform* and *Laplacian*) as shown in Table 1. The four groups of noise injections are arranged in descending orders of magnitudes for each of the seven process variables $\dot{E}_o$, $\dot{E}_{\eta n}$, $\dot{E}_{\eta p}$, $\dot{q}_{bn}$, $\dot{q}_{sn}$, $\dot{q}_{bp}$ and $\dot{q}_{sp}$ and each of the two sensor variables T_b and V. This means group 1 of injections represents the highest noise considered, while group 4 stands for the lowest noise.

The output estimated (by either the UKF or PF estimator) is denoted by $\hat{y}_i$. The performance measure of good estimation is the Root Mean Squared Error given by Equation (3.1):

$$RMSE = \sqrt{\frac{1}{n}\sum_{i=1}^{n}(y_i - \hat{y}_i)^2} \tag{3.1}$$

We summarize our simulation results in Table 2 to 4 for Gaussian, uniform and Laplacian noise injections, respectively. Each of these tables reports results for each of the aforementioned seven process variables and the two measurement variables and for each of the four groups of noise injections. For convenience we include in each of these tables the dB values of Injected Noise (IN). The tables are used to report the RMSE (in dB) for estimation *via* the Unscented Kalman Filter (UKF) and the Particle Filter (PF). Two observations are in order:

- For specific process or measurement variables, and a specific method of estimation, the RMSE decreases as one shifts from leftmost entires to rightmost ones, *i.e.*, from highest noise to lowest noise.

- The UKF estimation is definitely superior to the PF estimation in case of Gaussian noise and the $\dot{E}_{\eta p}$ variable. The PF estimator is more likely to perform better than the UKF estimator in case of uniform noise while for the Laplacian noise, the PF estimator dominantly outperforms the UKF estimator. We highlight in **bold** cases where the RMSE due to the PF is less than that of the UKF in Tables 3 and 4.

Tables 2 to 4 aggregate a performance measure (RMSE) for all pertinent variables. By contrast, Figs 1 to 12 detail the time behavior for the actual (measured), UKF estimation and PF estimation values of our most important variable, namely, the battery output voltage V. Figs 1 to 4 consider Gaussian noise, while Figs 5 to 8 explore uniform noise and Figs 9 to 12 demonstrate Laplacian noise. Each set of four figures for a specific noise type consider the four values of 10dB, 0dB, –10dB, and –20dB pertaining to the values of injected noise for the variable V in Groups 1, 2, 3 and 4, respectively, according to Table 1. Both estimators work very well and yield time functions indistinguishable from measured ones for all cases of the Gaussian noise (Table 1 to 4) and for the lower noise cases of uniform noise (Figs. 6 to 8) or Laplacian noise (Figs. 11 to 12). The deviations of the estimated curves from the measured one in Figs 5, 9 and 10 indicate that the PF estimator is generally better than the UKF estimator for uniform and Laplacian noise. These deviations are less pronounced for uniform noise than for Laplacian one. In fact, Fig. 9 (which has the most significant discrepancies of all figures) demonstrate a run-away divergent behavior of the UKF estimator, indicating instability for this estimator.

Table 2. Root mean squared error due to gaussian noise

	Highest Noise											Lowest Noise
	Group 1			Group 2			Group 3			Group 4		
	IN	UKF	PF	IN	UKF	PF	IN	UKF	PF	IN	UKF	PF
$\dot{E}_o$	–60	–27.39	–25.43	–70	–41.63	–36.99	–80	–50.60	–41.60	–90	–59.50	–46.93
$\dot{E}_{\eta n}$	–60	–18.71	–16.51	–70	–31.39	–27.82	–80	–40.37	–30.45	–90	–50.15	–35.98
$\dot{E}_{\eta p}$	–60	–38.17	–26.86	–70	–49.27	–36.42	–80	–59.98	–41.29	–90	–68.44	–45.67
$\dot{q}_{bn}$	10	15.25	21.49	0	1.31	8.49	–10	–8.23	2.87	–20	–18.62	–1.55
$\dot{q}_{sn}$	–10	5.86	11.90	–20	–8.08	–1.00	–30	–17.61	–6.62	–40	–27.96	–11.05
$\dot{q}_{bp}$	10	17.49	21.31	0	2.84	13.86	–10	–6.59	5.72	–20	–16.92	–0.46
$\dot{q}_{sp}$	–10	8.05	11.79	–20	–6.59	4.33	–30	–16.01	–3.76	–40	–26.31	–10.00
T_b	10	1.22	0.35	0	–9.60	–9.10	–10	–19.21	–18.93	–20	–29.30	–25.91
V	10	–17.46	–15.24	0	–30.29	–26.84	–10	–39.35	–29.44	–20	–49.40	–35.44

Table 3. Root mean squared error due to uniform noise

	Highest Noise											Lowest Noise
	Group 1			Group 2			Group 3			Group 4		
	IN	UKF	PF	IN	UKF	PF	IN	UKF	PF	IN	UKF	PF
$\dot{E}_o$	–60	**–17.88**	**–23.32**	–70	**–27.45**	**–29.05**	–80	**–37.13**	**–38.36**	–90	–47.14	–44.91
$\dot{E}_{\eta n}$	–60	**–7.77**	**–12.71**	–70	**–17.81**	**–20.17**	–80	–27.76	–26.17	–90	–37.82	–36.45
$\dot{E}_{\eta p}$	–60	–31.01	–30.02	–70	–39.91	–35.85	–80	–49.54	–41.63	–90	–59.53	–46.34
$\dot{q}_{bn}$	10	**26.39**	**23.03**	0	**16.70**	**14.69**	–10	6.81	10.23	–20	–3.25	0.97
$\dot{q}_{sn}$	–10	**16.97**	**13.40**	–20	**7.28**	**5.27**	–30	–2.60	0.63	–40	–12.66	–8.62
$\dot{q}_{bp}$	10	**29.17**	**20.11**	0	**18.96**	**19.04**	–10	**9.08**	**4.33**	–20	–1.00	2.09
$\dot{q}_{sp}$	–10	**19.70**	**10.73**	–20	9.50	9.55	–30	**–0.38**	**–5.24**	–40	–10.46	–7.40
T_b	10	**7.00**	**6.95**	0	**–3.08**	**–3.11**	–10	–13.05	–13.03	–20	–23.05	–22.96
V	10	**–6.66**	**–12.28**	0	**–16.36**	**–18.09**	–10	**–26.13**	**–26.48**	–20	–36.17	–34.90

Table 4. Root mean squared error due to laplacian noise

	Highest Noise											**Lowest Noise**
	Group 1			Group 2			Group 3			Group 4		
	IN	UKF	PF	IN	UKF	PF	IN	UKF	PF	IN	UKF	PF
$\dot{E}_o$	–60	**–11.83**	**–23.08**	–70	**–21.78**	**–25.91**	–80	**–31.19**	**–34.34**	–90	**–41.08**	**–42.11**
$\dot{E}_{\eta n}$	–60	**–1.98**	**–12.73**	–70	**–11.90**	**–16.29**	–80	**–21.69**	**–24.49**	–90	**–31.76**	**–33.92**
$\dot{E}_{\eta p}$	–60	–26.10	–25.27	–70	–34.59	–33.60	–80	–43.59	–41.16	–90	–53.46	–46.48
$\dot{q}_{bn}$	10	**32.15**	**20.75**	0	**22.45**	**16.64**	–10	**12.85**	**12.38**	–20	**2.82**	**2.79**
$\dot{q}_{sn}$	–10	**22.74**	**11.31**	–20	**13.03**	**7.29**	–30	**3.44**	**2.91**	–40	**–6.60**	**–6.64**
$\dot{q}_{bp}$	10	**37.20**	**18.47**	0	**24.63**	**20.61**	–10	**15.09**	**7.37**	–20	5.06	5.87
$\dot{q}_{sp}$	–10	**27.70**	**9.13**	–20	**15.17**	**11.15**	–30	**5.62**	**–1.95**	–40	–4.40	–3.63
T_b	10	**12.96**	**12.70**	0	2.89	3.03	–10	**–6.95**	**–6.96**	–20	**–16.96**	**–17.03**
V	10	**1.19**	**–12.21**	0	**–10.59**	**–14.93**	–10	**–20.15**	**–23.45**	–20	**–30.11**	**–31.901**

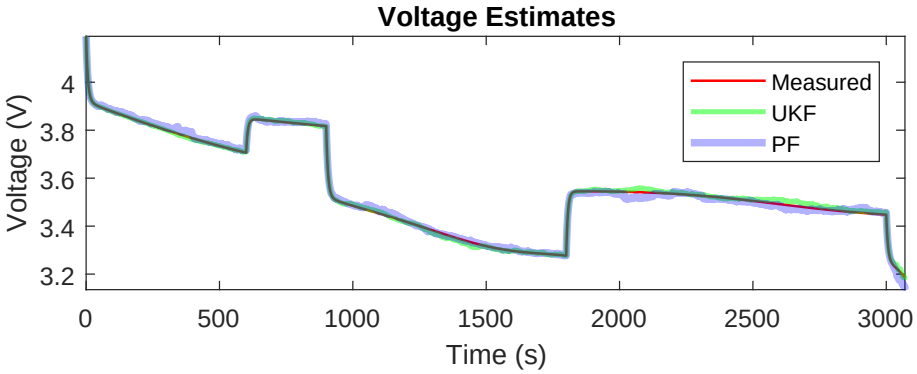

Fig. 1. Battery output voltage with gaussian noise of 10dB

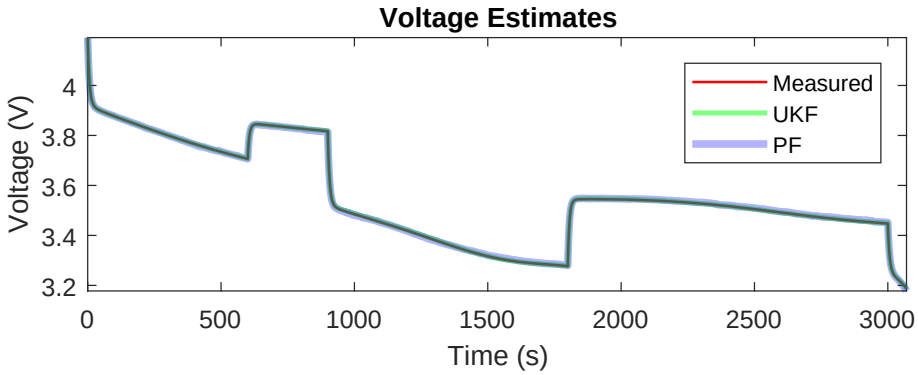

Fig. 2. Battery output voltage with gaussian Noise of 0dB

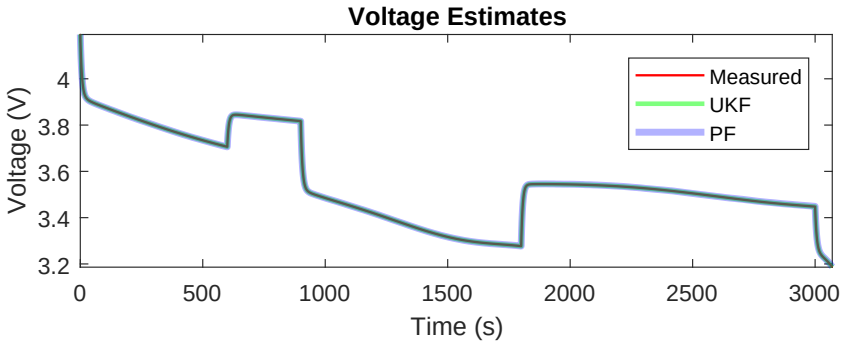

Fig. 3. Battery output voltage with gaussian noise of –10dB

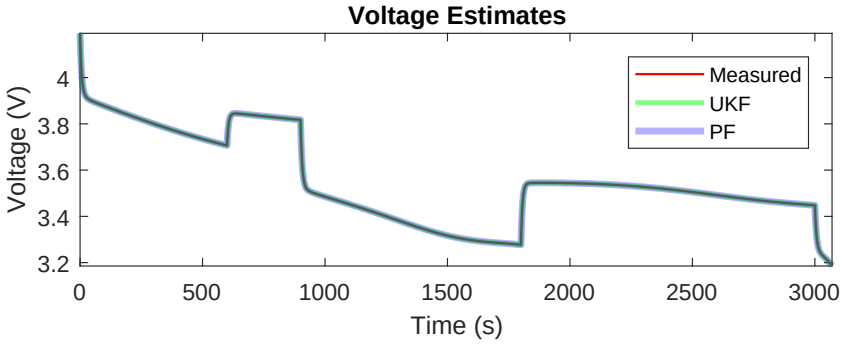

Fig. 4. Battery output voltage with gaussian noise of –20dB

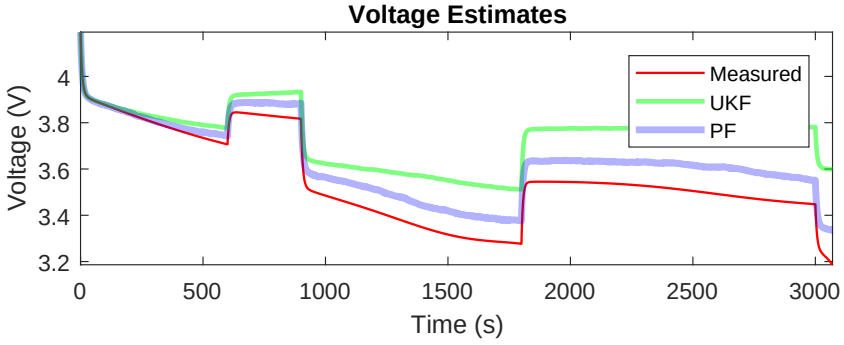

Fig. 5. Battery output voltage with uniform noise of 10dB

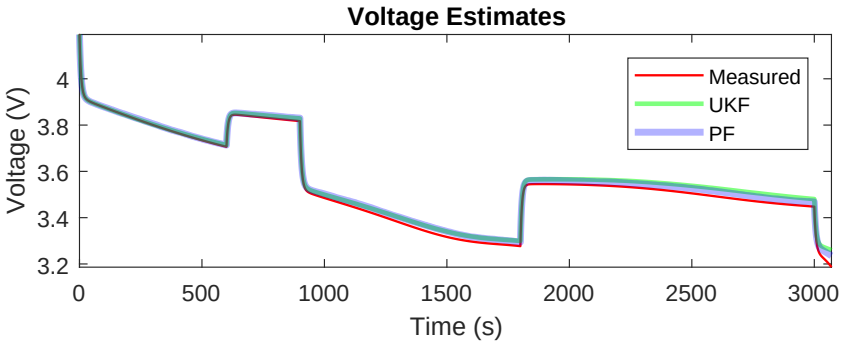

Fig. 6. Battery output voltage with uniform noise of 0dB

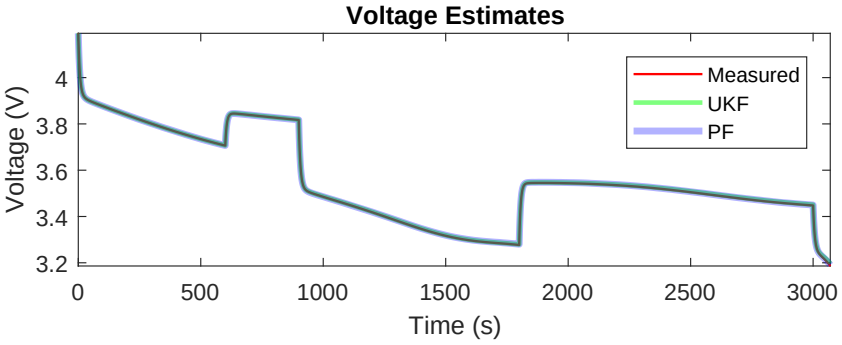

Fig. 7. Battery Output Voltage with Uniform Noise of −10dB

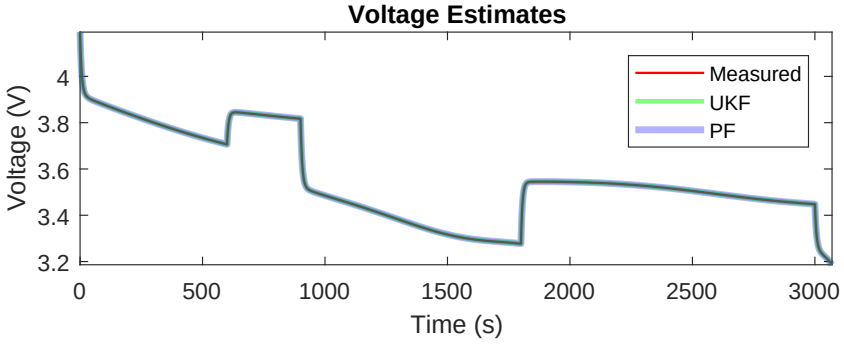

Fig. 8. Battery Output Voltage with Uniform Noise of −20dB

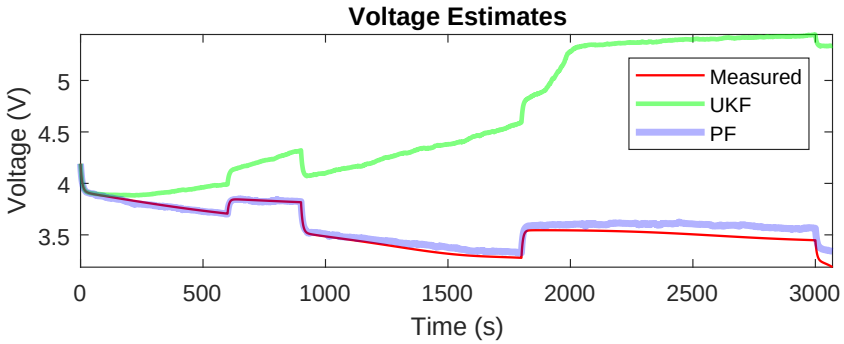

Fig. 9. Battery output voltage with laplacian noise of 10dB

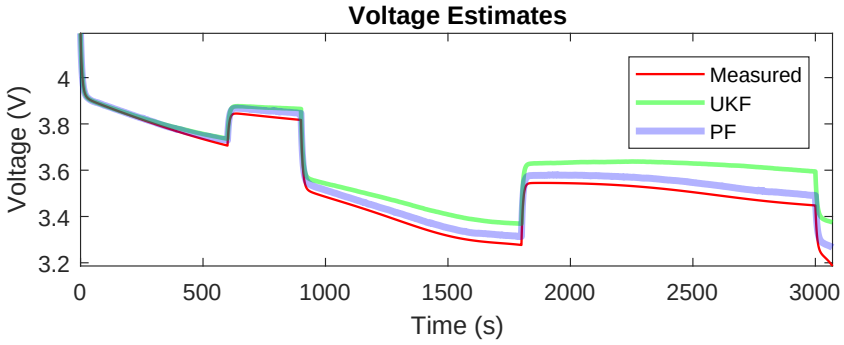

Fig. 10. Battery Output Voltage with Laplacian Noise of 0dB

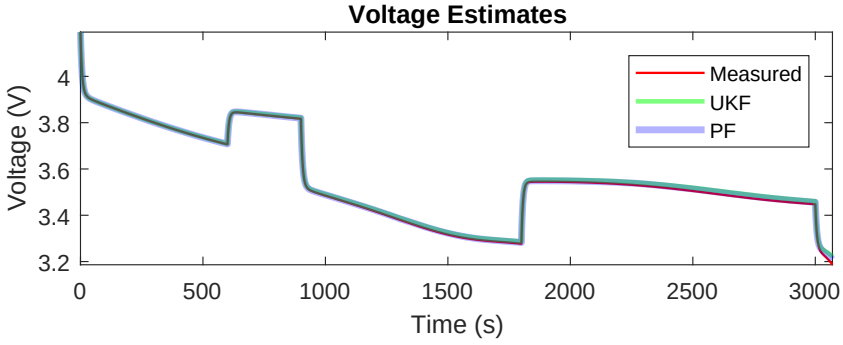

Fig. 11. Battery output voltage with laplacian noise of −10dB

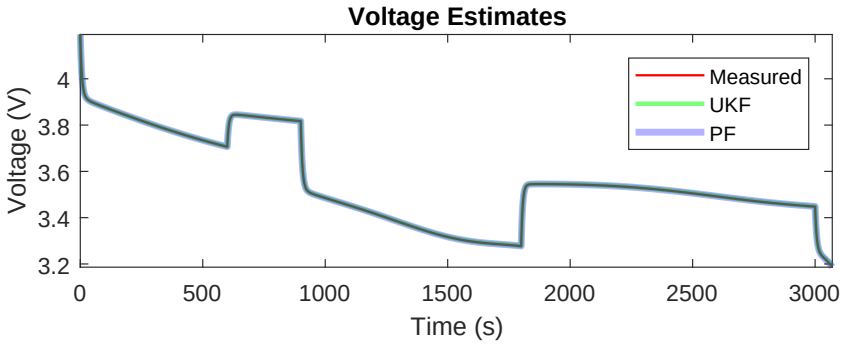

Fig. 12. Battery output voltage with laplacian noise of −20dB

4 Conclusion

This paper compared the detailed and aggregate dynamic performance for two estimators, *viz.*, the Unscented Kalman Filter (UKF) and the Particle Filter (PF), when applied to the state-space analysis of a noise-injected lithium-ion battery. The UKF outperformed the PF in the case of Gaussian noise injection. However, the PF was more or less better in the case of uniform noise, and even dominantly better in the case of Laplacian noise. The performance of both estimators deteriorated as the level of noise is increased, and a case of instability was identified with UKF estimation when high Laplacian noise is injected, wherein the UKF estimation exhibited a runaway divergent behavior. For future work, we hope to extend this work to cover other types of filters such as the Extended Kalman Filter (EKF), and also to include some heuristic or meta heuristic methods.

Acknowledgement

This article was funded by the Deanship of Scientific Research (DSR), King Abdulaziz University, Jeddah. The authors, therefore, acknowledge with thanks DSR technical and financial support.

Competing Interests

Authors have declared that no competing interests exist

References

[1] Lifeng Wu, Xiaohui Fu, Yong Guan. Review of the remaining useful life prognostics of vehicle lithium-ion batteries using data-driven methodologies. Applied Sciences. 2016;6(6):166.

[2] Aspasia Papazoglou, Stefano Longo, Daniel Auger, Francis Assadian. Nonlinear filtering techniques comparison for battery state estimation. Journal of Sustainable Development of Energy, Water and Environment Systems. 2014;2(3):259-269.

[3] Brian Bole, Chetan S. Kulkarni Matthew Daigle. Adaptation of an electrochemistry-based li-ion battery model to account for deterioration observed under randomized use. Proceedings of Annual Conference of the Prognostics and Health Management Society, Fort Worth, TX, USA. 2014;29.

[4] Matthew J. Daigle, Chetan Shrikant Kulkarni. Electrochemistry-based battery modeling for prognostics; 2013.

[5] Bhaskar Saha, Kai Goebel, Scott Poll, Jon Christophersen. An integrated approach to battery health monitoring using Bayesian regression and state estimation. Autotestcon, 2007 IEEE. 2007;646-653.

[6] Jiang J, Zhang C. Fundamentals and application of Lithium-ion batteries in electric drive vehicles. Wiley; 2015.

[7] Abbas Fotouhi, Daniel J. Auger, Karsten Propp, Stefano Longo Mark Wild. A review on electric vehicle battery modelling: From lithium-ion toward lithium–sulphur. Renewable and Sustainable Energy Reviews. 2016;56:1008-1021.

[8] Philip Ross. Boeing's battery blues [news]. Spectrum, IEEE. 2013;50(3):11-12.

[9] Bhaskar Saha, Kai Goebel. Modeling li-ion battery capacity depletion in a particle filtering framework. In Proceedings of the Annual Conference of the Prognostics and Health Management Society. 2009;2909-2924.

[10] Cheng Zhang, Kang Li, Lei Pei, Chunbo Zhu. An integrated approach for real-time model-based state-of-charge estimation of lithium-ion batteries. Journal of Power Sources. 2015;283:24-36.

[11] Cheng Zhang, Kang Li, Jing Deng, Shiji Song. Improved realtime state-of-charge estimation of lifepo4 battery based on a novel thermoelectric model. IEEE Transactions on Industrial Electronics. IEEE Transactions on Industrial Electronics. 2017;64(1):654-663.

[12] Gang Ning, Branko N. Popov. Cycle life modeling of lithium-ion batteries. Journal of the Electrochemical Society. 2004;151(10):A1584-A1591.

[13] Gang Ning, Ralph E. White, Branko N. Popov. A generalized cycle life model of rechargeable li-ion batteries. Electrochimica Acta. 2006;51(10):2012-2022.

[14] Matthew Daigle, Chetan S. Kulkarni. End-of-discharge and end-of-life prediction in lithium-ion batteries with electrochemistry-based aging models. In: AIAA Infotech@ Aerospace. 2016;2132.

[15] Simon J. Julier, Jeffrey K. Uhlmann. Unscented filtering and nonlinear estimation. Proceedings of the IEEE. 2004;92(3):401-422.

[16] Tudoroiu N, Sobhani-Tehrani E, Khorasani K. Interactive bank of unscented kalman filters for fault detection and isolation in reaction wheel actuators of satellite attitude control system. In: IEEE Industrial Electronics, IECON 2006-32nd Annual Conference, IEEE. 2006;264-269.

[17] Fei Zhang, Guangjun Liu, Lijin Fang. Battery state estimation using unscented kalman filter. In: Robotics and Automation, 2009. ICRA'09. IEEE International Conference, IEEE. 2009;1863-1868.

[18] Sanjeev Arulampalam M, Simon Maskell, Neil Gordon, Tim Clapp. A tutorial on particle filters for online nonlinear/non-gaussian bayesian tracking. IEEE Transactions on Signal Processing. 2002;50(2):174-188.

[19] Branko Ristic. Particle filters for random set models. Springer. 2013;798.

[20] Enrico Zio. Monte carlo simulation methods for reliability estimation and failure prognostics. In: Complex Data Modeling and Computationally Intensive Statistical Methods. Springer. 2010;151-164.

[21] Dawn An, Joo-Ho Choi, Nam Ho Kim. Prognostics 101: A tutorial for particle filter-based prognostics algorithm using matlab. Reliability Engineering & System Safety. 2013;115:161-169.

[22] Enrico Zio, Giovanni Peloni. Particle filtering prognostic estimation of the remaining useful life of nonlinear components. Reliability Engineering & System Safety. 2011;96(3):403-409.

[23] Arnaud Doucet, Adam M. Johansen. A tutorial on particle filtering and smoothing: Fifteen years later. Handbook of Nonlinear Filtering. 2009;12(656-704):3.

[24] Joaquín Klee Barillas, Jiahao Li, Clemens Günther, Michael A. Danzer. A comparative study and validation of state estimation algorithms for li-ion batteries in battery management systems. Applied Energy. 2015;155:455-462.

[25] Akbar Maleki, Fathollah Pourfayaz. Optimal sizing of autonomous hybrid photovoltaic/wind/battery power system with lpsp technology by using evolutionary algorithms. Solar Energy. 2015;115:471-483.

[26] Rui Xiong, Fengchun Sun, Zheng Chen, Hongwen He. A data-driven multi-scale extended kalman filtering based parameter and state estimation approach of lithium-ion olymer battery in electric vehicles. Applied Energy. 2014;113:463-476.

[27] Ho-Ta Lin, Tsorng-Juu Liang, Shih-Ming Chen. Estimation of battery state of health using probabilistic neural network. IEEE Transactions on Industrial Informatics. 2013;9(2):679-685.

[28] Nishi Swal, Vivek Shrivastava. An improve efficiency of li-ion batteries with harmony search algorithm. In: Energy Efficient Technologies for Sustainability (ICEETS), 2016 International Conference, IEEE. 2016;377-381.

[29] Scott J. Moura. Estimation and control of battery electrochemistry models: A tutorial. In: Decision and Control (CDC), 2015 IEEE 54th Annual Conference, IEEE. 2015; 3906-3912.

[30] Hasan Bjaili, Khalid Daqrouq, Rami Al-Hmouz. Speaker identification using bayesian algorithm. Trends in Applied Sciences Research. 2014;9(8):472.

[31] Fredrik Orderud. Comparison of kalman filter estimation approaches for state space models with nonlinear measurements. In: Proc. of Scandinavian Conference on Simulation and Modeling. 2005;1-8.

[32] Tamas L, Lazea Gh, Robotin R, Marcu C, Herle S, Szekely Z. State estimation based on kalman filtering techniques in navigation. In: Automation, Quality and Testing, Robotics, 2008. AQTR 2008. IEEE International Conference, IEEE. 2008;2:147-152.

[33] Grewal MS, Andrews AP. Kalman Filtering: Theory and Practice with MATLAB. Wiley - IEEE. Wiley; 2015.

[34] Bruce P. Gibbs. Advanced Kalman filtering, least-squares and modeling: A practical handbook. John Wiley & Sons; 2011.

© *2017 Bjaili et al.; This is an Open Access article distributed under the terms of the Creative Commons Attribution License (http://creativecommons.org/licenses/by/4.0), which permits unrestricted use, distribution, and reproduction in any medium, provided the original work is properly cited.*

Peer-review history:
The peer review history for this paper can be accessed here (Please copy paste the total link in your browser address bar)
http://sciencedomain.org/review-history/19645